Published in J. Vac. Sci. Technol. B 21 1812 (2003).

Plasma-assisted molecular beam epitaxy of GaN on porous SiC substrates with varying porosity

Ashutosh Sagar, C. D. Lee and R. M. Feenstra
Department of Physics, Carnegie Mellon University, Pittsburgh, Pennsylvania, 15213
C. K. Inoki and T. S. Kuan
Department of Physics, University at Albany, SUNY, Albany, New York, 12222

Abstract: We have grown GaN on porous SiC substrates and studied the effect of substrate porosity on the overgrown film quality in terms of defect structure and density and film strain. The growth was performed by plasma-assisted molecular beam epitaxy (PAMBE). The GaN films were characterized by x-ray, transmission electron microscopy (TEM) and wafer curvature measurements by surface profilometry. TEM images show that the GaN film grown on porous substrates contains open tubes and a low dislocation density in regions between tubes. We discuss various growth mechanisms that can lead to these defect features in the GaN film. However, we do not find any overall improvement in the x-ray rocking curve FWHM of the GaN films grown on porous substrates compared to those on nonporous substrates. It was found that the GaN films grown on porous SiC were significantly more strain relaxed compared to those grown on nonporous substrate. We propose various mechanisms that can lead to the reduction in strain in GaN films grown on porous substrates and compare the data with finite element analysis (FEA) simulations of such a system.

I. Introduction

There has been considerable interest in recent years in using porous (ps) SiC as a substrate to grow epitaxial SiC and GaN with reduced dislocation density [1-6]. Porous SiC is prepared by anodizing n-type SiC in hydrofluoric acid (HF) under ultra-violet illumination [7]. Earlier studies of the growth of GaN on porous SiC substrates have shown an improved GaN film quality [2,3,4,8]. It was found that the GaN film on porous SiC was more strain relaxed and had a reduced dislocation density by a factor of two compared to those grown on nonporous substrates [8].

It has been speculated that a porous surface may serve as a template for nano-scale lateral epitaxial overgrowth (nano-LEO) [4] in GaN, and that a porous substrate layer may be compliant to lattice and thermal mismatch strains [2-4]. In this work, we discuss the possible mechanisms which may give rise to such effects and their effectiveness in dislocation density reduction and strain relaxation in our samples. We have grown GaN films on porous SiC surfaces with different porosities, under nominally identical conditions, to study the effect of surface pore density on the overgrown GaN film quality. The GaN film was characterized by x-ray and transmission electron microscopy (TEM) to study the dislocations and the amount of strain relaxation. In addition, we measured the surface curvature of the films to evaluate their biaxial strain.

We present the results of a finite element analysis (FEA) simulation to estimate the effectiveness of porous layer in absorbing the thermal mismatch strain in the GaN film and compare it with substrates whose porous morphologies consist of either vertical pillars or vertical pores.

II. Experiment

The porous SiC samples used in this study were purchased from TDI, Inc. They were prepared by anodic etching at current density of 7 mA/cm^2 for 3 min, with a 250 W Hg lamp illuminating the 2 in. diameter wafers. All our samples, used in this study, were 6H polytype with a 3.5° miscut angle. The MBE growth of GaN was performed on the (0001) face of the porous SiC samples in Ga rich conditions, as described elsewhere [8].

Figure 1(a) shows a plan-view scanning electron microscope (SEM) image of a typical porous SiC surface. The surface pores are 20-50 nm wide. We described the morphology of the bulk porous layer in a previous work [9]. In that paper, we showed that the pores start to form on the surface and then grow in a highly connected, dendritic fashion in the bulk. Thus, the porosity of the surface is much smaller than the bulk porous layer. There exists a thin nonporous skin layer, typically ≈ 50 nm thick, at the surface where the porosity is considerably less than that of the bulk [9]. As was reported earlier, reactive ion etching (RIE) in SF_6 gas can be used to remove the skin layer and thus increase the surface porosity without affecting the bulk porous structure [9]. We have used this RIE process to increase the surface porosity of our samples so that, combined with the non-RIE samples, we have a wide range of samples with different surface porosities.

Hydrogen etching is often used to remove polishing damage from SiC wafers, thereby producing atomically flat surfaces needed for epitaxy [10]. During hydrogen etching, the sample is heated to about 1700°C in hydrogen atmosphere. In our present study, we hydrogen etched all our samples briefly (1 minute) at 1700°C. It was found that the hydrogen etching affects the pore size, making them bigger [9]. For example, Fig. 1(a) shows nano size (20 – 50 nm) pores in a plan-view SEM image of an as-received porous SiC sample. Fig. 1(b) is an image of the same sample after it has been hydrogen etched for 1 minute. Fig. 1(c) shows another image of a sample from the same wafer, which was reactive ion etched in SF_6 plasma for 6 minutes and then hydrogen etched for 1 minute. Figure 1(d) show an SEM image of a different sample which was not reactive ion etched but was only hydrogen etched for 1 minute. The surface porosity of our samples was measured simply by counting the number of surface pores after the hydrogen etching. The surface pore density of the samples in Fig. 1(b), (c) and (d) was 3.5, 13 and 11.5 μm^{-2}, respectively. Using this combination of RIE and hydrogen etching, we prepared a range of samples with different surface porosities as needed for the present study.

After the hydrogen etching, samples were loaded into the MBE chamber. GaN growth was performed in Ga rich condition at the substrate temperature 750°C. A nitrogen plasma cell was used for nitrogen source and the growth proceeded for 8 hours with estimated growth rate of about 0.2 μm/hr. After the growth, samples were characterized by x-ray by measuring the FWHM of the symmetric (0002) and asymmetric $(10\bar{1}2)$ rocking curves to estimate screw and threading dislocation density in the films. Subsequently, we measured the curvature of the GaN film by a stylus profiler. As discussed in a later section, the surface curvature of the film was used to calculate the biaxial strain in GaN film. TEM images were taken in cross section to study the dislocations in the GaN film.

III. Results and discussion

A. Dislocation density

Figure 2(a) shows a cross sectional TEM images of a GaN film grown on nonporous SiC and Figs. 2(b) and (c) show TEM images of GaN films grown on porous SiC substrates. The GaN film of Fig. 2(b) was grown on the porous SiC surface whose plan view image is shown in Fig. 1(c). As mentioned earlier, that substrate was reactive ion etched in SF_6 for 6 minutes before being hydrogen etched for 1 minute, and the resulting surface pore density was 13 μm^{-2}. As seen in Figs. 2(b) and (c), after the GaN growth, the substrate pores are generally filled with Ga droplets. We also find that GaN nucleates on the pore walls close to the substrate surface and then grows laterally. Such local GaN LEO process caps some of the pore openings. However, at the openings that are only partially closed by LEO, open tubes can extend vertically all the way to the top surface of the film. Most of these tubes are filled with Ga. In regions between these tubes, dislocation half loops are seen to punch in horizontally from the tube walls [Fig. 2(b)]. This result is in contrast to Fig. 2(a), where the dislocations are mostly created and propagated from the film/substrate interface.

Figure 2(c) shows GaN film grown on a different porous substrate, whose surface is shown in Fig. 1(d). The surface pore density in this case is 11.5 μm^{-2}, similar to that of Fig. 1(c), but the surface morphology is significantly more planar between the pores and the average size of the pores is smaller than that of Fig. 1(c). This flatter surface morphology is evident in the TEM image of Fig. 2(c). We also observe there open tubes originated from essentially all pores at the substrate surface and extended up through the film, suggesting that lateral overgrowth of GaN has not occurred on such flat pored surface. Here again the dislocation density in between the tubes is low, with most dislocations being half-loops gliding in from the open tubes in the GaN.

Figure 3 shows a plot of symmetric and asymmetric rocking curve FWHM of GaN film as a function of substrate pore density. On average, there does not seem to be any significant improvement in the x-ray FWHM for the films grown on the various porous substrates. In fact, the x-ray FWHM shows an increasing trend with the increase in surface pore density of the substrate. Since the x-ray FWHM is a measure of the average strain variations in a large area of the film (due to the beam size ~1 mm^2) and also through the entire thickness of the GaN film, this value does not give us a true picture of the defect structure and growth mechanisms working at the nano scale. Even though x-ray results are not significantly improved for growth on the porous substrates, TEM images show that the porous substrate is able to produce areas in the GaN film having low defect density.

B. Thermal strain reduction

Since the GaN and the SiC have different coefficients of thermal expansion, the GaN film on SiC develops a thermal strain when the sample is cooled down from the growth temperature to the room temperature [11]. It was shown elsewhere that the GaN film after cool down is under compressive strain [11]. This strain results in the surface curvature of the GaN film and can be calculated by measuring this curvature. If the radius of curvature of the film is R, and the Young's modulus of the substrate and film are M_{sub} and M_{film} respectively, then the biaxial strain in the film is given by [12]

$$\varepsilon_{xx} = M_{sub} \bullet t_{sub}^2 / (6 \bullet M_{film} \bullet t_{film} \bullet R),$$

where t_{sub} and t_{film} denote the thickness of the substrate and the film respectively. We used M_{sub} = 586 GPa and M_{film} = 479 GPa for SiC and GaN, respectively [11].

We measured the curvature of our samples by stylus profilometry. Figure 4 shows a plot of strain in the GaN film as a function of the surface pore density on the SiC substrate. The inset in the Fig. 4 shows several curves from the stylus profiler. The negative sign in strain corresponds to a film under compression. It is clear from the plot that the porous substrates have a dramatic effect on reducing the GaN film strain. The GaN film grown on nonporous SiC substrates is under compressive strain whereas the films grown on the porous substrates are almost strain free, and in one case, under tension (That particular data point in Fig. 4, along with with a neighboring one, are marked with a "P" and were obtained from samples grown as part of a previous study [8]).

Regarding the observed reduction in film strain, we first note that all the samples grown on the porous layer show a very similar strain reduction (except for one of the samples from the previous study with tensile strain, mentioned above). This result implies that the strain reduction may be a property of the bulk porous layer and not the surface pore density. Also, we point out that due to lower thermal conductivity of the porous SiC compared to the nonporous SiC, the growth temperature on the porous SiC, for a given substrate heater power, is about $\sim 40^0$ C higher than that of the nonporous substrate [13]. This temperature difference in the porous SiC substrate results in a film with a reduced Ga/N ratio on its surface during growth, and such films could display different residual stress because of different dislocation density or some other effect. However, for the films grown for the present study (*i.e.* not including those marked "P" in Fig. 4), we adjusted the sample heater power during growth in an attempt to compensate for the temperature difference. The sample temperature was measured by an optical pyrometer and the heater power was adjusted so that the temperature read by the pyrometer was the same for all samples. We tentatively conclude that a growth temperature difference is *not* the origin of the observed strain reduction. Rather, it may arise from a difference in dislocation density in the films grown on porous compared to nonporous substrates, with an increased dislocation density in the former case implying a reduction in strain at the growth temperature.

Another possible mechanism for strain relaxation is that the porous SiC substrate and possibly the tube-containing GaN film may be more compliant to absorb the film strain during the cool down process [14-16] than the solid film and substrate. In other words, the porous layer (and/or the film) may behave like a mechanically flexible buffer layer under the GaN film. During the cool down process, this porous layer would deform itself, absorbing the GaN film stress as a compliant substrate and thus finally producing a strain free GaN film. However, since the porous network is a highly interconnected network, it is questionable whether this layer can be flexible enough to act like a compliant substrate. This question has been previously raised for SiGe heteroepitaxy on Si [17], where a comparison of porous morphology to that of nano-size pillars was considered. Intuitively, it seems that the pillars can more easily deform and better act like a compliant substrate than a porous layer. To address this issue, we have performed finite element analysis (FEA) simulations of these two kinds of surfaces to see how

effectively can the porous layer serve as a compliant substrate and produce a strain-free epitaxial film.

Figures 5(a) and (b) show two FEA models of a surface with pillars and pores respectively. For simplicity, the pores were square shaped vertical wells. The substrate in this case was 30 units wide. The compliant layer with pillars or pores was 10 units thick on top of a solid substrate that was 100 units thick. The epitaxially grown layer is 30 units thick on top of the pillars or pores. We assume that, at the growth temperature, the GaN grows pseudomorphically (i.e. without any lattice mismatch) on SiC [18]. When the sample is cooled down to room temperature, the GaN and SiC lattice constants are reduced to 3.19 and 3.08 Å respectively (room temperature values of a-axis) resulting in 3.4 % lattice mismatch between the GaN and 6H-SiC [11]. In our simulations, we apply this strain by starting with the system strain free at a temperature T_1 and then cooling it down to a temperature T_2. The difference in the thermal expansion coefficient between GaN and SiC ($\Delta\alpha$) times the temperature difference $\Delta T = T_1 - T_2$, was taken to be $\Delta\alpha\Delta T = -0.034$ so that a corresponding strain developed in the system.

Figures 5(c) and (d) show the simulated system after cool down. We find that both pillars and pores act as compliant layers, relieving the strain in the film. This effect is seen most strongly in Fig. 5(c), where the strain is constant (*i.e.* nearly zero) throughout the film. In Fig. 5(d) a varying strain field is evident in the film, as seen of the curved film sides immediately above the porous layer. However the porosity of this porous layer is only half that of the layer with pillars used in Fig. 3(c). For a constant porosity of the pillars and pores we find that, within a factor of 2, they produce similar amounts of strain relaxation in the film. Though this model of the porous layer is rather simple compared to an actual porous network in a real sample, the results from the simulation show that a porous layer can in principle act like compliant substrate thereby reducing strain in the overgrown film. It should, however, be pointed out that the simulations were done on a relatively small sample size (ratio of the porous layer to the sample width was 1/3 for the results shown in Fig. 5). In a real case, when the ratio of the porous layer to the sample size is very small ($\sim 10^{-4}$), the effect of such a compliant substrate mechanism will be reduced because of the large lateral (shear) deflection needed in the porous layer to absorb that strain. Simulations to study these effects are currently underway.

At present we cannot make a definitive conclusion regarding the possible compliant nature of the porous substrate and/or open tubes in the GaN. However, it seems likely that the observed strain reduction in the GaN films on porous substrates *will* be affected by the increased dislocation density in those films (*i.e.* at the growth temperature, the films on porous substrates may have lower strain than for the growth on nonporous substrates, and this difference is preserved as the films are cooled). X-ray rocking curves of our samples, as shown in Fig. 3, indicate that the overall dislocation density does increase with the increasing surface porosity, and this increase in the dislocation density can lead to strain relaxation. The half loop dislocations gliding in from the tubes in the GaN film, as seen in Figs. 2 (b) and 2(c), may provide one particular source of strain relaxation. These half loop dislocations are not seen in the GaN films grown on nonporous substrates.

IV. Conclusions

In this work, we have grown GaN on porous SiC substrates using plasma-assisted molecular beam epitaxy. We showed with cross sectional TEM images that the GaN films on porous SiC substrates have regions of low dislocation density. It was seen in several cases that the GaN film on porous SiC has open tubes extending over the substrate pores. We also observed instances of lateral epitaxial overgrowth in GaN films over the porous substrates and dislocations terminating at the tube walls in the film. However, we did not find any overall improvement in the FWHM of the symmetric and asymmetric rocking curves on these GaN films grown on substrates with different porosities. We found that that GaN film grown on the porous SiC substrates is strain relaxed compared to those grown on nonporous substrates and we discussed different models that can lead to the relaxed GaN film on porous substrates. Finite element analysis simulations were performed to confirm that a porous layer can indeed act like a compliant substrate and absorb the overgrown film strain, at least for the small wafer diameters considered in the simulations.

Acknowledgements

This work was supported by a Defense University Research Initiative on Nanotechnology (DURINT) program administered by the Office of Naval Research under Grant N00014-01-1-0715 (program monitor C. Wood).

REFERENCES:

1. S. E. Saddow, M. Mybaeva, W. J. Choyke, S. Bai, G. Melnychuk, Y. Koshka, V. Dmitriev and C. E. C. Wood, Materials Science Forum **353-356**, 115 (2001).
2. M. Mynbaeva, A. Titkov, A. Kryzhanovski, V. Ratnikov, H. Huhtinen, R. Laiho and V. Dmitriev, Appl. Phys. Lett. **76**, 1113 (2000).
3. M. Mynbaeva, A. Titkov, A. Kryzhanovski, I. Kotousova, A. S. Zubrilov, V. V. Ratnikov, V. Yu. Doavydov, N. I. Kuznetsov, K. Mynbaev, D. V. Tsvetkov, S. Stepanov, A. Cherenkov, and V. Dmitriev, MRS Internet J. Nitride Semicond. Res. **4**, 14 (1999).
4. M. Mynbaeva, A. Titkov, A. Kryzhanovski, A. Zubrilov, V. Ratnikov, V. Doavydov, N. Kuznetsov, K. Mynbaev, S. Stepanov, A. Cherenkov, A. Kotousova, D. Tsvetkov, V. Dmitriev, Mat. Res. Soc. Symp. Vol. 595, W2.7.1 (2000).
5. G. Melnychuk, M. Mynbaeva, S. Rendakova, V. Dmitriev and S. E. Saddow, Mat. Res. Soc. Symp. Vol. 622, T4.2.1 (2000)
6. X. Li, Y. –W. Kim, P. W. Bohm, I. Adesida, Appl. Phys. Lett. **80**, 980 (2002).
7. J. S. Shor, I. Grimberg, B. –Z. Weiss and A. D. Kurtz, Appl. Phys. Lett. **62**, 2836 (1993).
8. C. K. Inoki, T. S. Kuan, C. D. Lee, A. Sagar and R. M. Feenstra, D. D. Koleske, D. J. Diaz, P. W. Bohn, and I. Adesida, submitted to J. Electron. Mat.
9. A. Sagar, C. D. Lee, R. M. Feenstra, C. K. Inoki, and T. S. Kuan, J. Appl. Phys., **92**, 4070 (2002).
10. V. Ramachandran, M. F.Brady, A. R. Smith, and R. M. Feenstra, J. Electron. Mat.**27**, 308 (1998).
11. B. J. Skromme, H. Zhao, D. Wang, H. S. Kong, M. T. Leonard, G. E. Bulman, and R. J. Molnar, Appl. Phys. Lett. **71**(6), 829 (1997).
12. M. Doerner and W. Nix, CRC Critical Reviews in Sol. State and Mat. Sci. **14**, 224 (1998).
13. This temperature difference between the porous and nonporous samples is apparent from the results of GaN growth on SiC, in which the GaN on the porous side had a morphology indicative of lower surface coverage of Ga. An identical change in the surface morphology can be achieved by a $\approx 40^0$ C increase in the sample temperature which increases the Ga desorption rate from the surface. [C. D. Lee, V. Ramachandran, A. Sagar, R. M. Feenstra, D. W. Greve, W. L. Sarney, L. Salamanca-Riba, D. C. Look, Song Bai, W. J. Choyke R. P. Devaty, J. Electron. Mat. **30**, 162, (2001)].
14. Z. Yang, F. Gaurin, I. W. Tao, W. I. Wang, and S. S. Iyer, J. Vac. Sci. Technol. B, **13** (2), 789 (1995).
15. C. Carter-Coman, A. S. Brown, N. M. Jokerst, D. E. Dawson, R. Bicknell-Taussius, Z. C. Feng, K. C. Rajkumar, and G. Dagnall, J. Elec. Mat. **25** (7), 1044 (1996).
16. D. Zubia and S. D. Hersee, J. Appl. Phys. **85** (9), 6492 (1999).
17. Y. H. Xie and J. C. Bean, J. Appl. Phys. **67** (2), 792 (1990).
18. Our initial condition of pseudomorphic growth is not realistic since the films are certainly, at least partially, strain relaxed at the growth temperature. However, for the purpose of the FEA simulations, this assumption provides an adequate starting point.

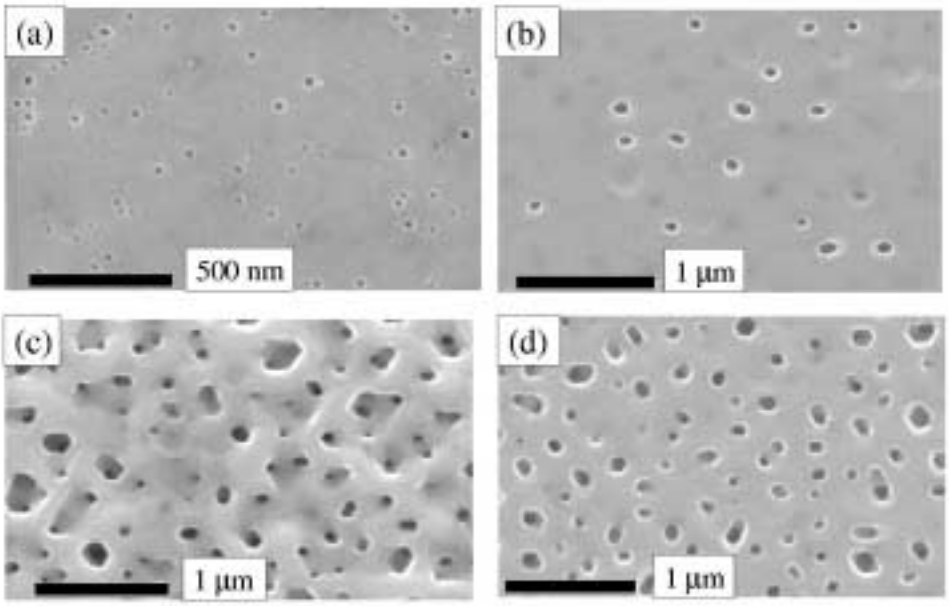

Figure 1. Plan view scanning electron microscope (SEM) images of porous SiC surfaces: (a) as-received porous surface without any surface etching treatment, (b) the surface after hydrogen etching for 1 min at 1700^{o}C, (c) the surface after reactive ion etching in SF_6 for 6 minutes followed by hydrogen etching for 1 minute at 1700^{o}C. Images (a)-(c) refer to the same wafer, after various processing steps. Image (d) is from a different wafer, prepared by hydrogen etching at 1700^{o}C for 1 minute.

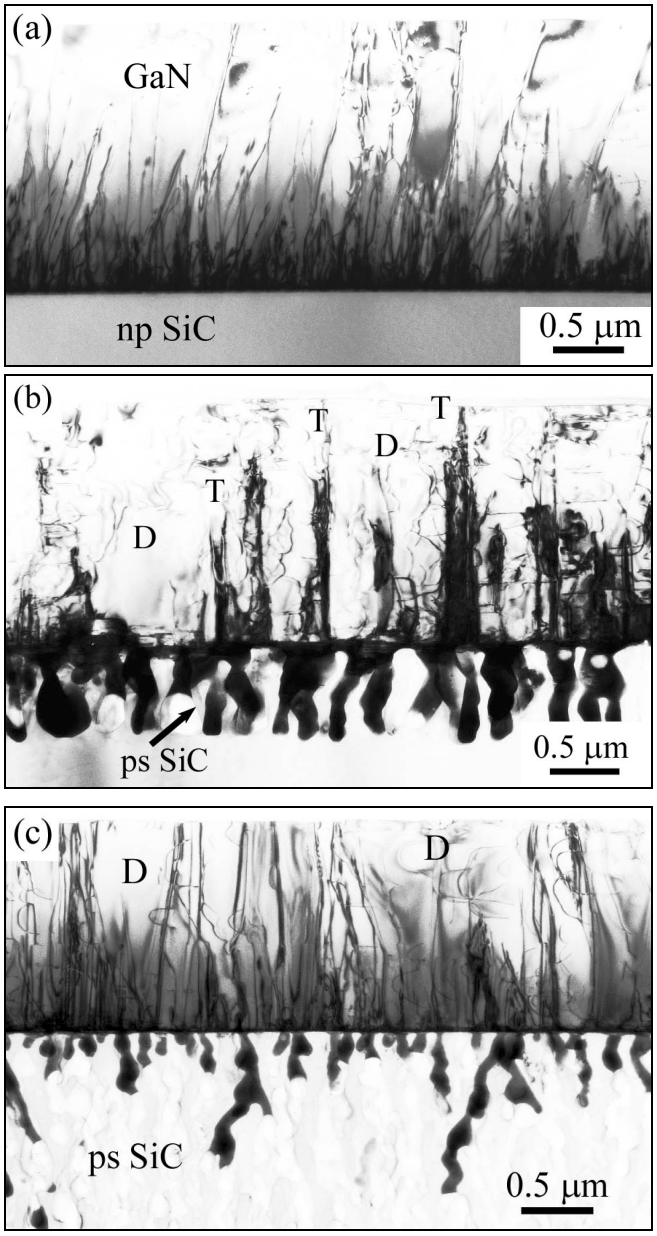

Figure 2. Cross sectional TEM images of GaN film on (a) nonporous SiC substrate, and (b) and (c) porous SiC substrates. The surface pore density of the substrate in (b) is 13 μm^{-2} [see Fig. 1(c)] and in (c) is 11.5 μm^{-2} [see Fig. 1(d)]. The regions labeled by D in (b) and (c) contain a low density of dislocation half loops gliding in from tubes, some of them marked by T.

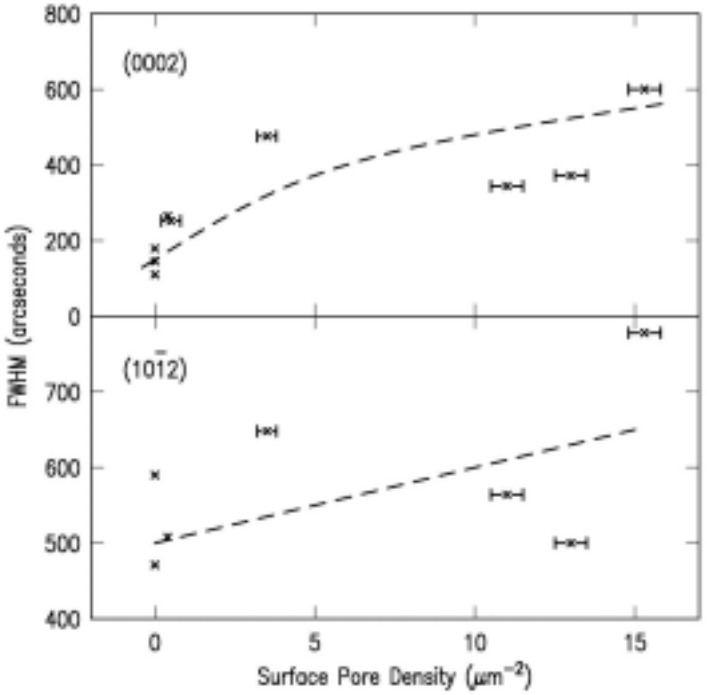

Figure 3. Triple axis symmetric and asymmetric x-ray rocking curve FWHM of the GaN films grown on porous SiC. The abscissa in the above plots shows the number of surface pores on various substrates. The dashed lines are drawn as guides to the eye.

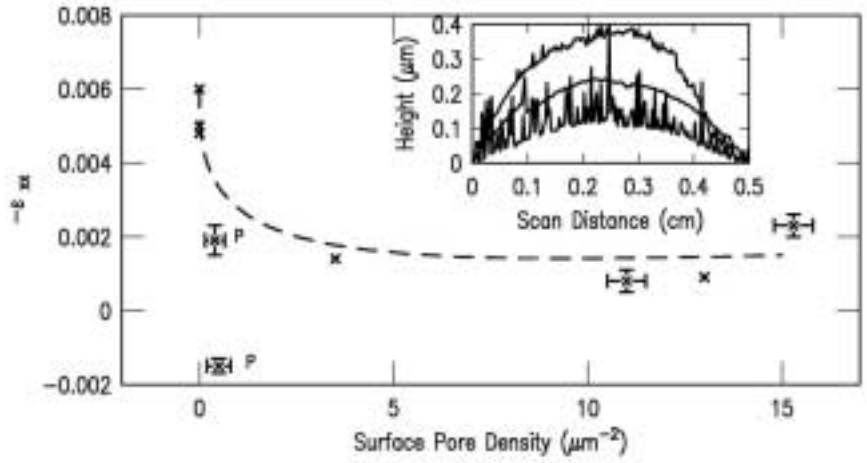

Figure 4. In-plane strain in the GaN film, determined from the film curvature, as a function of surface pore density of the SiC substrate. Negative strain means that the film is in compression. The presence of pores on the substrate is seen to have a dramatic effect in reducing the film strain. The inset shows some of the surface curvature plots measured by stylus profilometry. The dashed line is drawn as a guide to the eye. Error bars are shown at typical data points. The data points marked "P" were from samples grown in for a previous study (Ref. [8]); all other points were obtained from samples grown for the present study.

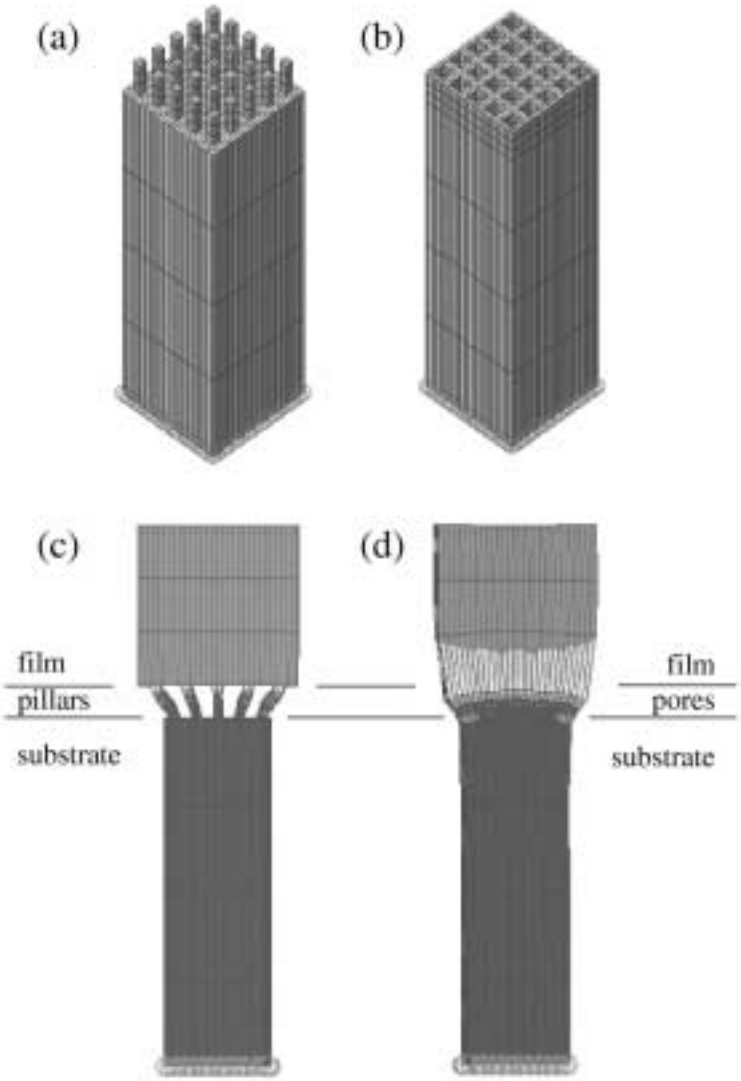

Figure 5. Finite element analysis models used to study the compliant nature of a substrate for absorbing the thermal mismatch between the substrate and the overgrown film. Two different types of compliant substrates were studied, containing (a) pillars (with width of 2 units on a 6 unit base, resulting in 88.8% porosity) and (b) pores (with wall thickness of 2 units on a 6 unit base, resulting in 44.4% porosity). Panel (c) shows the film on the pillars after it has been cooled down and panel (d) shows the film on pores after the same amount of cooling. Displacements are shown with ×10 magnification, and the gray scale is shaded according to the in-plane component of the strain.